JOURNAL OF VIROLOGY, May 2006, p. 4546–4556 Vol. 80, No. 9
0022-538X/06/$08.00+0 doi:10.1128/JVI.80.9.4546–4556.2006

Prion Infection of Oral and Nasal Mucosa

Crista DeJoia, Brian Moreaux, Kimberly O'Connell, and Richard A. Bessen*

Department of Veterinary Molecular Biology, Montana State University, Bozeman, Montana 59717

Received 10 December 2005/Accepted 16 February 2006

Centrifugal spread of the prion agent to peripheral tissues is postulated to occur by axonal transport along nerve fibers. This study investigated the distribution of the pathological isoform of the protein (PrP^{Sc}) in the tongues and nasal cavities of hamsters following intracerebral inoculation of the HY strain of the transmissible mink encephalopathy (TME) agent. We report that PrP^{Sc} deposition was found in the lamina propria, taste buds, and stratified squamous epithelium of fungiform papillae in the tongue, as well as in skeletal muscle cells. Using laser scanning confocal microscopy, PrP^{Sc} was localized to nerve fibers in each of these structures in the tongue, neuroepithelial taste cells of the taste bud, and, possibly, epithelial cells. This PrP^{Sc} distribution was consistent with a spread of HY TME agent along both somatosensory and gustatory cranial nerves to the tongue and suggests subsequent synaptic spread to taste cells and epithelial cells via peripheral synapses. In the nasal cavity, PrP^{Sc} accumulation was found in the olfactory and vomeronasal epithelium, where its location was consistent with a distribution in cell bodies and apical dendrites of the sensory neurons. Prion spread to these sites is consistent with transport via the olfactory nerve fibers that descend from the olfactory bulb. Our data suggest that epithelial cells, neuroepithelial taste cells, or olfactory sensory neurons at chemosensory mucosal surfaces, which undergo normal turnover, infected with the prion agent could be shed and play a role in the horizontal transmission of animal prion diseases.

The lymphoreticular and nervous systems are pathways for prion agent replication and transport to the brain. Oral ingestion of the prion agent leads to deposition of the disease-specific isoform of the prion protein (PrP^{Sc}) in the alimentary and gut-associated lymphoid tissue as well as the enteric nervous system of sheep and cervids (1, 27, 54). Spread of the prion agent to the spinal cord and brain stem occurs via transport by the sympathetic and parasympathetic divisions of the autonomic nervous system (6, 7, 34, 53). Additional spread of the prion agent within the lymphoreticular system (LRS) leads to prion infection of secondary lymphoid organs throughout the host. The LRS has long been known to be a site of prion agent replication and a pathway to infection of the nervous system, but studies of experimental rodent models have established that LRS infection is not always required for neuroinvasion from peripheral sites (33, 43). One study has demonstrated that prion infection of densely innervated peripheral tissues could result in direct prion neuroinvasion (4).

The pathways involved in the centripetal spread of the prion agent following oral ingestion have been well defined, but less is known about centrifugal spread of the prion agent in pathogenesis. Dissemination of the prion agent from the brain and spinal cord to peripheral tissues is postulated to be due to anterograde transport of PrP^{Sc} along nerve fibers. Studies investigating transport of the cellular prion protein (PrP^{C}) in central and peripheral axons demonstrate both anterograde and retrograde axonal transport (10, 38); a similar mechanism may explain PrP^{Sc} transport in prion diseases. Evidence for centripetal and centrifugal transport of the Creutzfeldt-Jakob disease (CJD) agent along the optic nerve is provided by cases of iatrogenic CJD that have been linked to corneal transplants (16, 26). In the recipient host the prion agent spreads from the transplanted cornea to the brain, while in the donor the host agent likely spreads centrifugally from the brain to the cornea. Demonstration of the prion agent in the retina (24, 50), trigeminal ganglion (21, 52), and facial nerve (12) in human or animal prion diseases also supports the hypothesis that the prion agent can spread away from the brain via several distinct cranial nerves, assuming that oral ingestion of the prion agent results in centripetal spread to the central nervous system in these hosts. In sheep with natural scrapie, the presence of PrP^{Sc} in muscle spindles of the tongue (3) is suggestive of centrifugal spread of the scrapie agent along the trigeminal nerve to these sensory spindles. Previous studies of experimental prion infection of hamsters demonstrate spread of the prion agent to skeletal muscles in the tongue and other areas after oral and intracerebral inoculation (5, 49). These findings support the hypothesis that the prion agent can undergo anterograde transport along the hypoglossal nerve to skeletal muscles in the tongue. This view is further supported by colocalization of PrP^{Sc} to nerve fibers and the neuromuscular junction in the tongues of hamsters infected with the HY strain of the transmissible mink encephalopathy (TME) agent (39), suggesting that the prion agent can spread across the neuromuscular junction in order to establish infection in muscle.

Transmission of animal prion diseases is by both vertical and horizontal routes, but the source(s) of prion infectivity in horizontal spread has not been firmly established. Vertical transmission of the scrapie agent in sheep has been postulated to be due to postpartum contamination with scrapie-infected placenta (2, 42), but additional studies indicate a low level of prion infectivity in blood (29), which may imply a role for in utero transmission of scrapie. Horizontal prion transmission in sheep and cervids is less likely to involve blood-borne routes, although prion-infected placental tissues or blood shed into

* Corresponding author. Mailing address: Department of Veterinary Molecular Biology, P.O. Box 173610, Montana State University, Bozeman, MT 59717. Phone: (406) 994-1563. Fax: (406) 994-4303. E-mail: rbessen@montana.edu.

TABLE 1. Primary antibodies and their specificity used to investigate HY TME infection by laser scanning confocal microscopy

Antibody target	Class (dilution)	Antibody specificity in tongue	Source (location)	Reference(s)
Prion protein	Monoclonal 3F4 (1/400)	Prion protein with 3F4 epitope	Gift from Victoria Lawson	32
α-Gustducin	Polyclonal (1/200)	Type II taste cells	Santa Cruz Biotechnology (Santa Cruz, CA)	11, 63
Synaptobrevin-2	Polyclonal (1/200)	Type II and III taste cells; intragemmal and subgemmal nerve fibers	Wako Chemicals (Richmond, VA)	62
SNAP-25	Polyclonal (1/200)	Type III taste cells; some intragemmal nerve fibers	Calbiochem (San Diego, CA)	61
Protein gene product 9.5	Polyclonal (1/2,000)	Neuronal cell bodies and axons in CNS and periphery; some type II and III taste cells	Biogenesis (Brentwood, NH)	30, 64
Protein gene product 9.5	Monoclonal (1/400)	Neuronal cell bodies and axons in CNS and periphery; some type II and III taste cells	Biogenesis (Brentwood, NH)	60
Cytokeratin	Polyclonal (1/800)	Keratins in all epithelial layers; neuroepithelial cells	Dako Cytomation (Carpinteria, CA)	46

pasture could account for environmental contamination. Studies investigating environmental sources of prion transmission in chronic wasting disease (CWD) indicate that paddocks contaminated by excreta from CWD-positive mule deer or decomposed carcasses of mule deer naturally infected with CWD can transmit CWD infection to sentinel deer (36). The high prevalence of CWD (e.g., >15%) in areas of endemicity in Colorado and Wyoming and the high penetrance of CWD (~90%) in cervid research stations suggest that this disease can be efficiently transmitted between susceptible hosts (35, 59). To date, prion infectivity has not been described in saliva, nasal secretions, respiratory aerosols, urine, or feces in naturally occurring prion infections. However, prion excretion in urine has recently been demonstrated in studies using prion-infected transgenic mice with chronic lymphocytic inflammation of the kidney (47). These findings indicate that superimposed disease processes may alter the sites of PrP^{Sc} accumulation to tissues not previously known to harbor PrP^{Sc}.

In the current study we investigated the centrifugal spread of the prion agent to the oral and nasal mucosae of hamsters in order to examine potential sites of prion agent shedding from epithelial surfaces. Hamsters were intracerebrally inoculated with the HY TME agent, and the location of PrP^{Sc} was investigated in the tongue and nasal cavity. Laser scanning confocal microscopy revealed that PrP^{Sc} was found in nerve fibers, taste cells, and the stratified squamous epithelium in fungiform papillae of HY TME-infected hamsters. PrP^{Sc} deposition was also identified in the olfactory and vomeronasal sensory epithelia, and its distribution was consistent with HY TME infection of sensory neurons. These findings indicate that the HY TME agent can undergo centrifugal spread to the oral and nasal mucosa via gustatory, somatosensory, or olfactory nerve fibers and subsequently spread to neuroepithelial or epithelial cells via peripheral synapses. This study suggests that horizontal prion transmission of scrapie and CWD could be linked to the continual turnover and/or shedding of prion-infected taste cells, epithelial cells, or olfactory sensory neurons into mucus or saliva.

MATERIALS AND METHODS

Animal inoculations and tissue collection. All procedures involving animals were approved by the Montana State University Animal Care and Use Committee and were in compliance with the *Guide for the Care and Use of Laboratory Animals*. Weanling Syrian golden hamsters (Charles River Laboratories, Boston, MA) were intracerebrally inoculated with 50 μl of a brain homogenate from a normal hamster (i.e., mock infected) or a TME-infected hamster containing $10^{7.8}$ intracerebral median lethal doses per milliliter of the HY TME agent as previously described (8, 9). Following inoculation with the HY TME agent, hamsters were observed three times per week for the onset of clinical symptoms, which include hyperexcitability, head tremors, and ataxia. Animals were euthanized in the early stages of clinical disease.

PrP^{Sc} immunohistochemistry. For PrP^{Sc} analysis, tongue, brain, and skulls containing the nasal cavity were collected and PrP^{Sc} immunohistochemistry (IHC) was performed as previously described (5). Briefly, animals were intracardially perfused with paraformaldehyde-lysine-periodate fixative followed by immersion fixation in the same fixative for 5 h, except skulls, which were immersion fixed for 24 h. Following immersion fixation, tongues were cut midsagittally for processing and embedding. The nasal cavity was cut into anterior, midturbinate, and posterior cross sections prior to embedding. All soft tissue was removed from the skulls, and they were immersed in a 10% EDTA-tetrasodium solution until they were decalcified. Following dehydration, tissues were embedded in paraffin and cut into 5-μm-thick sections. Tissues from a minimum of three animals per group were analyzed. A minimum of 40 sections throughout the thickness of the tissue was examined per animal. All tissue sections were subjected to antigen retrieval by treatment with formic acid (99%, wt/vol) for 10 min, followed by 6 M guanidine thiocyanate for 10 min. Tissue sections were successively incubated with anti-PrP monoclonal 3F4 antibody (Table 1) overnight at 4°C, and then incubated with horse anti-mouse biotinylated secondary antibody (1:400; Vector Laboratories, Burlingame, CA) at room temperature for 30 min, followed by streptavidin-horseradish peroxidase (1:500; Biosource International, Camarillo, CA) at room temperature for 20 min. PrP^{Sc} was visualized with 3-amino-9-ethylcarbazole in 50 mM sodium acetate with H_2O_2 added to a final concentration of 0.012%. Tissue sections were mounted with Aquamount (Lerner Laboratories, Pittsburgh, PA) and placed under coverslips for viewing with a Nikon Eclipse E600 bright-field microscope. Controls for PrP^{Sc} IHC included the use of mock-infected tissues and substitution of a murine immunoglobulin G (IgG) isotype control for the primary anti-PrP 3F4 monoclonal antibody.

PrP^{Sc} dual immunofluorescence. PrP^{Sc} immunofluorescence staining was combined with immunofluorescence for the cell-type-specific markers PGP 9.5, SNAP-25, α-gustducin, synaptobrevin-2, and cytokeratin (Table 1). For the PrP^{Sc} dual-immunofluorescence procedure, the streptavidin-horseradish peroxidase in the incubation step in PrP^{Sc} IHC was replaced with Alexa Fluor 488 streptavidin conjugate (Molecular Probes, Portland, OR) at a 1:400 dilution. The rabbit polyclonal antibodies to cell-type-specific markers were visualized by incubation with goat anti-rabbit Alexa Fluor 568 antibody (1:200; Molecular Probes, Portland, OR). The nuclear counterstain ToPro-3 (Molecular Probes, Portland, OR) was applied to some tissue sections at a concentration of 0.25 μM for 10 min. Controls for immunofluorescence included mock-infected tissues and replacement of the primary antibodies with an IgG isotype control. Tissue sections were placed under coverslips with Mowiol mounting medium (51). Tissues from a minimum of three HY TME-infected animals and three mock-infected animals were examined. A minimum of 50 sections throughout the thickness of the tissue

was examined for each tongue per cell-type-specific immunofluorescence experiment. For each cell-type-specific and PrP^{Sc} dual-immunofluorescence study, a minimum of 32 fungiform papillae were analyzed from HY TME-infected hamsters.

Confocal laser scanning microscopy. Images were visualized using a Zeiss LSM 510 Meta confocal system equipped with a Zeiss Plan-Apochromat 63×, 1.40-NA oil objective. Double immunofluorescence was imaged after excitation of the Alexa Fluor 488 with an argon laser at a wavelength of 488 nm and excitation of Alexa Fluor 568 with a helium-neon laser at a wavelength of 543 nm. Images were scanned sequentially to minimize cross talk between channels, and each line was scanned four times and averaged to increase the signal-to-noise ratio. The pinhole aperture was adjusted so that each channel had an optical slice of 0.8 μm. The channels could then be combined into a single image for quantitative analysis.

Deconvolution of confocal images. Deconvolution was performed using Huygens Essential software (version 2.7; Scientific Volume Imaging, Hilversum, The Netherlands). The point spread function of the Zeiss LSM 510 Meta confocal microscope was measured using images of fluorescent latex beads (diameter, 175 nm) captured at the same image parameters as the images for analysis. Multiple bead images were averaged, and this average was utilized as the point spread function for deconvolution. Using the cropping tool, the region of interest (e.g., taste bud, lamina propria, stratified squamous epithelium) within the image was chosen for deconvolution. A maximum likelihood estimation algorithm was applied to deconvolve the confocal images. Signal-to-noise ratio was determined as the maximum intensity over average background, which was estimated by the software for a three-dimensional region with the lowest average value in the image. For each dual-immunofluorescence experiment, a minimum of 10 image stacks from three hamsters that were captured at 0.25-μm intervals through the *z* axis of the tissue were analyzed.

Colocalization analysis of confocal images. Deconvolved images were evaluated for colocalization using the Colocalization Analyzer tool of the Huygens Essential software, which provides information about the amount of spatial overlap between structures in different data channels. Colocalization coefficients were generated by the analyzer module, including the Manders overlap coefficient (MOC) and M1 and M2 coefficients. The MOC indicates the overlap of signals in image pairs and is insensitive to differences in signal intensities between two channels, photobleaching, or amplifier settings. It has a value range of 0 to 1, with a value of 0 indicating no colocalization and a value of 1 indicating that all pixels in both channels colocalize. An additional analysis was performed on HY TME-infected tissues by division of the MOC into two different subcoefficients, termed M1 and M2. These coefficients are calculated for pixel intensity ranges defined by an area of interest in the image and are insensitive to differences in signal intensities. The coefficient M1 is used to describe the contribution of channel 1 (i.e., cellular marker immunofluorescence) to the colocalized area, while M2 is used to describe the contribution of channel 2 (i.e., PrP^{Sc} immunofluorescence) to the colocalized area.

Statistical analysis. The average MOCs of the confocal images generated from the HY TME-infected tissues were compared to the average MOCs of the images generated from mock-infected tissues to evaluate the probability (*P* value) that the colocalization observed in the experimental samples was greater than would be expected by chance. Statistical comparisons of MOCs were performed using Student's *t* test for data sets passing the normality test or the Mann-Whitney rank sum test for data sets failing the normality test on SigmaStat software (version 3.0; SYSTAT Software, Inc., Richmond, CA). A P value of <0.05 was considered to be statistically significant, and M2 values for HY TME were reported only when a statistical difference was found between results for mock- and HY TME-infected tissues.

RESULTS

To investigate the centrifugal spread of the prion agent to mucosal tissue, the cellular location of PrP^{Sc} was examined in the tongues of hamsters that were intracerebrally (i.c.) inoculated with the HY TME agent. PrP^{Sc} IHC in the tongues of clinically ill hamsters revealed PrP^{Sc} deposition in three specific regions: fungiform papillae that are widely distributed on the dorsal surface of the rostral tongue, skeletal muscle cells, and nerve fibers (Fig. 1). Eighty percent of the fungiform papillae ($n = 49$) had evidence of PrP^{Sc} deposits, and these were found in the lamina propria, taste bud, or stratified squamous epithelium (SSE). The majority of PrP^{Sc} accumulation in the fungiform papillae was observed in the lamina propria, which contains sensory nerve fibers that innervate the taste cells and surrounding epithelium. PrP^{Sc} immunostaining was identified in discrete nerve fascicles in the lamina propria directly beneath the taste bud, both in longitudinal and cross-sectional orientations. Punctate PrP^{Sc} immunostaining was also present within the taste bud at both apical and basal locations (Fig. 1D) and in the SSE that is located lateral and apical to the taste bud (Fig. 1B, arrowhead). Ninety-one percent of taste buds ($n = 26$) in fungiform papillae had evidence of PrP^{Sc} deposition following i.c. inoculation with the HY TME agent. PrP^{Sc} accumulation was rarely present in the stratum corneum, although punctate staining was often present at the apical portion of the stratum granulosum. A distinct morphological transition between the stratum corneum and stratum granulosum was not always apparent. Fungiform papillae that did not contain discernible taste buds also exhibited PrP^{Sc} immunostaining in the lamina propria and SSE. However, no PrP^{Sc} deposition was observed in the SSE of filiform papillae (data not shown), which are distributed over the entire dorsal surface of the tongue and do not contain taste buds. Other sites of PrP^{Sc} deposition in the tongue parenchyma included nerve fascicles (Fig. 1E) and skeletal muscle cells (Fig. 1F). PrP^{Sc} immunostaining was less frequent in skeletal muscle, and PrP^{Sc}-positive muscle cells were usually surrounded by PrP^{Sc}-negative muscle cells. No PrP^{Sc} immunostaining was observed in the tongues of mock-infected hamsters (Fig. 1C) or in HY TME-infected tongue samples immunoreacted with mouse IgG control antibody (data not shown).

To investigate HY TME infection in the peripheral nerves of the hamster tongue, laser scanning confocal microscopy (LSCM) was used to determine the spatial relationship of PrP^{Sc} and nerve fibers in fungiform papillae following i.c. inoculation of the HY TME agent. The fungiform papillae receive specialized sensory innervation from the chorda tympani branch of the facial nerve and somatosensory innervation from the lingual nerve, which is a branch of the mandibular division of the trigeminal nerve. Previous studies have demonstrated that chorda tympani fibers innervate taste buds, while the lingual fibers ascend to the SSE lateral to the taste buds in fungiform papillae of hamsters (58). Immunofluorescence with anti-protein gene product 9.5 antibody (PGP 9.5) (Table 1) showed extensive innervation of the fungiform papillae in the lamina propria, especially below the base of the taste bud, an area referred to as the subgemmal plexus (Fig. 2A). PGP 9.5 immunofluorescence was also found at basal and apical locations in the taste bud, indicating the presence of nerve fibers and type II or III taste cells, as these neuroepithelial cells are also PGP 9.5 immunopositive (64). PGP 9.5-immunopositive nerve fibers were observed ascending to the SSE lateral to the taste bud (Fig. 2A). PrP^{Sc} immunofluorescence on the same tissue sections demonstrated PrP^{Sc} deposition in similar regions of the fungiform papillae, especially in the taste bud (i.e., intragemmal) and in the subgemmal plexus, with smaller amounts of PrP^{Sc} in the SSE (Fig. 2B). Colocalization of PrP^{Sc} and PGP 9.5 by LSCM revealed extensive areas of PrP^{Sc} overlap with PGP 9.5 in the lamina propria, taste bud, and SSE, but there were also areas where no overlap of the two markers was observed (Fig. 2C).

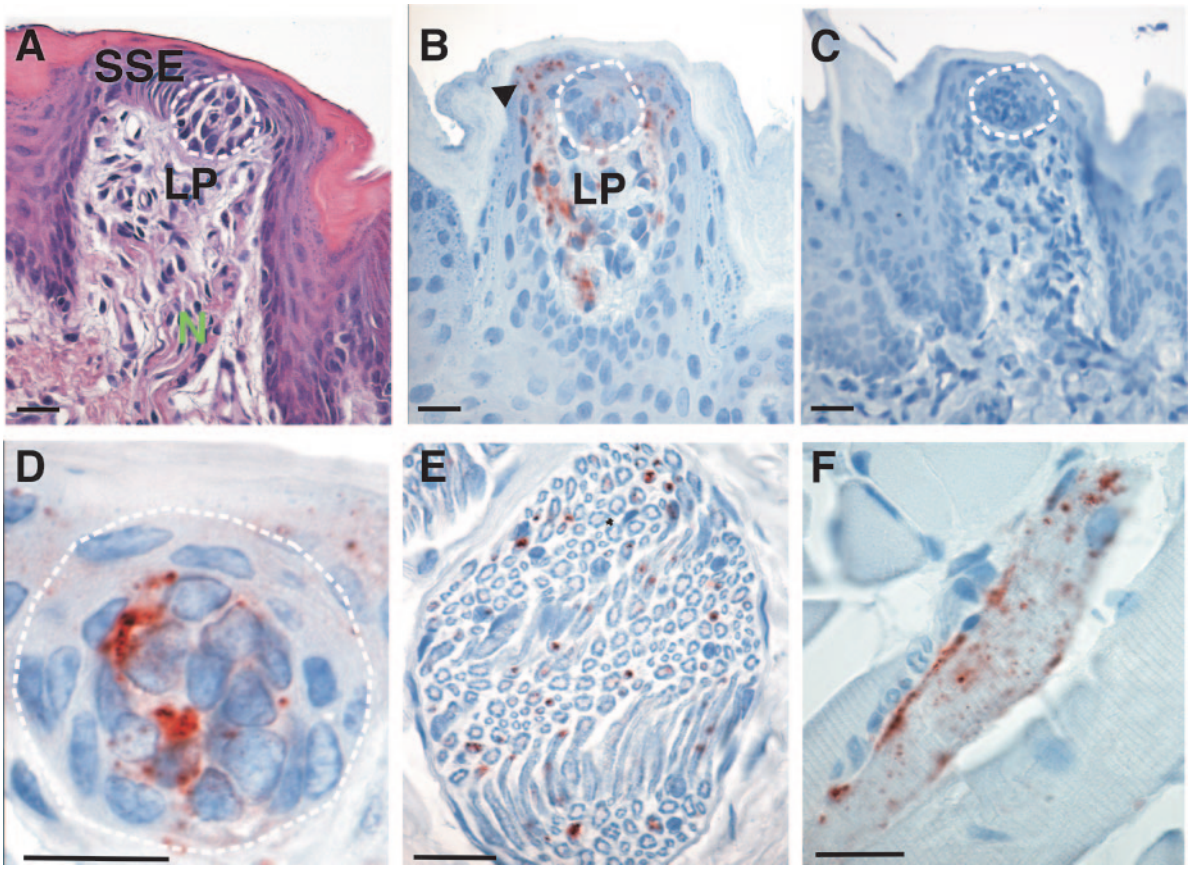

FIG. 1. PrP^{Sc} deposition in tongue following intracerebral inoculation of the HY TME agent. PrP^{Sc} immunohistochemistry in clinical HY TME-infected (B, D, E, and F) and asymptomatic mock-infected (C) hamsters is shown. PrP^{Sc} (red punctate staining) deposits (B and D) were present in taste bud, lamina propria, stratified squamous epithelium, and nerve fibers in the fungiform papillae of clinically ill hamsters but not in tongues of mock-infected hamsters (C). In the tongue parenchyma, PrP^{Sc} deposits were present in nerve fascicles (E) and skeletal muscle (F). Following PrP^{Sc} immunohistochemistry, tissue was counterstained with hematoxylin (B through F). The taste bud in the fungiform papilla is outlined with a dashed line (A through D) based on morphology. A filled arrowhead (B) indicates PrP^{Sc} deposits in the stratified squamous epithelium. Specific structures in fungiform papillae are identified in a hematoxylin-and-eosin-stained section (A). LP, lamina propria; N (in gray lettering), nerve fiber in lamina propria. Bar, 25 μm.

A quantitative analysis of PrP^{Sc} and PGP 9.5 colocalization in fungiform papillae was performed on confocal images of mock-infected and HY TME-infected tissues using Huygens software deconvolution and colocalization analysis. A comparison of MOCs between mock-infected and HY TME-infected tissues showed a difference between animal groups ($P < 0.001$, Mann-Whitney rank sum test) in colocalization of PrP^{Sc} and PGP 9.5 in the lamina propria, taste bud, and SSE (Table 2). The differences in colocalization between the mock- and HY TME-infected groups demonstrate that the overlap observed is not a random event, since PrP^{Sc} is not found in mock-infected tissue. The M1 and M2 coefficients, which indicate the relative contributions of channel 1 (red; PGP 9.5) and channel 2 (green; PrP^{Sc}) fluorophores to the colocalized area, were also calculated for each region in the HY TME-infected group. The M2 colocalization coefficient is important to the current analysis since it represents the contribution of PrP^{Sc} to the colocalized area. The M2 values for the lamina propria and SSE regions were 0.78 and 0.73, respectively (Table 2). Thus, 78% and 73% of PrP^{Sc} colocalized with PGP 9.5 in these tissue areas in HY TME-infected tongue. The taste bud region had an M2 value of 0.36, indicating that 36% of the PrP^{Sc} seen in this region was contained in either nerve fibers, type II taste cells, or type III taste cells (Table 2). These studies revealed that the fungiform papillae are densely innervated and that the HY TME agent can spread to nerve fibers and/or neuroepithelial cells in the lamina propria, taste bud, or SSE following infection of the brain.

To determine the cellular location of PrP^{Sc} in taste buds of fungiform papillae following i.c. inoculation of the HY TME agent, LSCM was performed using three taste-cell-specific markers: α-gustducin (type II taste cells), synaptobrevin-2 (type II and III taste cells), and SNAP-25 (type III taste cells) (Table 1). LSCM for PrP^{Sc} and synaptobrevin-2 (Fig. 3B) revealed a difference ($P = 0.005$, Student's t test) in MOCs between mock-infected and HY TME-infected hamsters in the taste bud region (Table 2). The M2 coefficient in HY TME-infected taste buds indicated that 52% of the PrP^{Sc} located within the taste bud region overlapped with synaptobrevin-2-labeled cells. Colocalization of PrP^{Sc} and α-gustducin, a marker for type II taste cells, did not reveal overlap by LSCM (Fig. 3A) or by MOC analysis ($P = 0.29$, Mann-Whitney rank

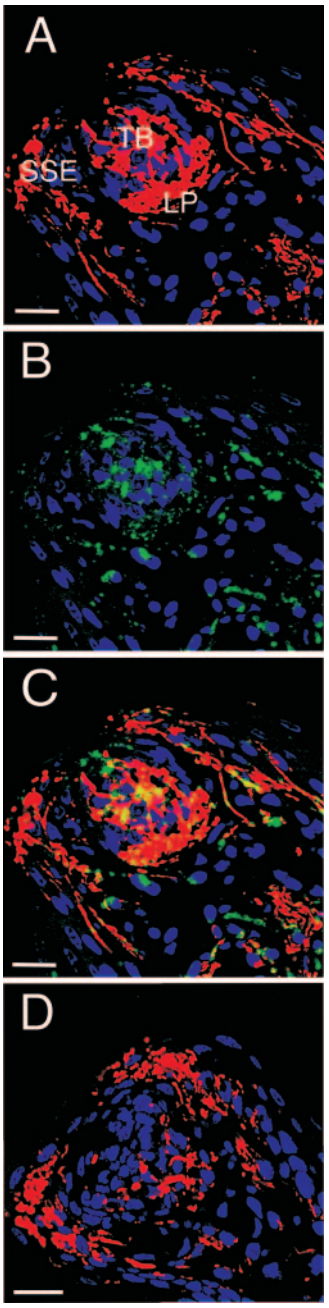

FIG. 2. Laser scanning confocal microscopy for PGP 9.5 and PrP^{Sc} in the fungiform papillae of hamsters intracerebrally inoculated with the HY TME agent. Immunofluorescence images for PGP 9.5 (A, red) and PrP^{Sc} (B, green) on the same tissue section were merged to illustrate areas of overlap (C, yellow). ToPro-3 (blue) was used as a nuclear counterstain. During the clinical phase of TME disease, colocalization of PGP 9.5 and PrP^{Sc} was found in the taste bud and lamina propria, with a lesser amount in the stratified squamous epithelium. No PrP^{Sc} immunofluorescence was found in the fungiform papillae of mock-infected hamsters following dual immunofluorescence for PGP 9.5 and PrP^{Sc} (D). LP, lamina propria; TB, taste bud. Bar, 20 μm. Images have an optical thickness of 0.8 μm.

sum test) in the taste buds of mock- and HY TME-infected hamsters. Comparison of PrP^{Sc} colocalization with SNAP 25-positive (type III) taste cells (Fig. 3C) between mock-infected and HY TME-infected taste buds showed a difference in MOCs ($P < 0.001$, Student's t test) while the M2 coefficient in the taste bud region of HY TME-infected hamsters indicated that 44% of PrP^{Sc} in the taste bud overlapped with this type III taste cell marker (Table 2). The lack of PrP^{Sc} colocalization with α-gustducin (type II taste cells) and the presence of colocalization with both synaptobrevin-2 (type II and III taste cells) and SNAP-25 (type III taste cells) suggested that PrP^{Sc} was not found in type II taste cells but was present in type III taste cells. It should be noted that both synaptobrevin-2 and SNAP-25 are also found in some intragemmal nerve fibers (61, 62), and PrP^{Sc} colocalization with these markers could indicate a distribution in nerve fibers, which is consistent with PrP^{Sc} colocalization with PGP 9.5 in the taste bud region (Fig. 2C and Table 2). There was no colocalization of PrP^{Sc} and SNAP-25 in the lamina propria of fungiform papillae, an area that does not contain taste cells (Table 2). In summary, PrP^{Sc} deposits in the taste bud colocalized with markers for type III taste cells but did not colocalize with markers for type II taste cells; this finding could be important with respect to prion agent spread if hamster type III taste cells synapse with gustatory nerve fibers, as has been reported in the taste cells of the rat (64).

To investigate the cellular location of PrP^{Sc} in the SSE of the hamster tongue following i.c. inoculation of the HY TME agent, LSCM was performed on tissue incubated with an antibody to cytokeratin, which is a marker for keratins that are present in the SSE and taste cells. Cytokeratin immunofluorescence revealed uniform staining of the stratum granulosum and stratum corneum; the signal extended from the edge of the lamina propria to the apical end of the papillae (Fig. 4A). PrP^{Sc} immunofluorescence on the same tissue sections revealed PrP^{Sc} deposition in the SSE of fungiform papillae that was prominent in the lateral apical regions (Fig. 4B). LSCM for both PrP^{Sc} and cytokeratin revealed that the majority of PrP^{Sc} in the SSE

TABLE 2. Colocalization of PrP^{Sc} and cell-type-specific markers in HY TME-infected hamster tongue

Antibody[a]	Region[b]	Average overlap coefficient (MOC)[c]		HY TME M2 coefficient[d]
		Mock	HY TME	
PGP 9.5	LP	0.017 ± 0.008	0.147 ± 0.023*	0.78
SNAP-25	LP	0.185 ± 0.082	0.083 ± 0.027	NA
Synaptobrevin-2	LP	0.045 ± 0.149	0.223 ± 0.063*	0.65
PGP 9.5	TB	0.005 ± 0.003	0.081 ± 0.012*	0.36
SNAP-25	TB	0.022 ± 0.008	0.097 ± 0.013*	0.44
Synaptobrevin-2	TB	0.037 ± 0.009	0.134 ± 0.028*	0.52
α-Gustducin	TB	0.049 ± 0.015	0.033 ± 0.012	NA
PGP 9.5	SSE	0.021 ± 0.007	0.148 ± 0.011*	0.73
SNAP-25	SSE	0.007 ± 0.003	0.014 ± 0.010	NA
Synaptobrevin-2	SSE	0.068 ± 0.020	0.131 ± 0.025	NA
Cytokeratin	SSE	0.031 ± 0.007	0.077 ± 0.004*	0.95

[a] Antibodies used in conjunction with anti-PrP monoclonal 3F4 antibody for confocal microscopy studies.

[b] Confocal images were cropped to either the lamina propria (LP), taste bud (TB), or stratified squamous epithelium (SSE) for colocalization analysis.

[c] Overlap coefficient after Manders ± standard error of the mean, $n = 10$. *, $P \leq 0.005$, using Student's t test or the Mann-Whitney rank sum test. A P value of <0.05 indicated a significant difference between the mock- and HY TME-infected groups.

[d] Colocalization coefficient M2 indicates the percentage of PrP^{Sc} that overlaps with the cell-type-specific marker in the region of analysis in HY TME-infected hamster tongue. NA, not applicable since there was no statistical difference between HY TME- and mock-infected groups.

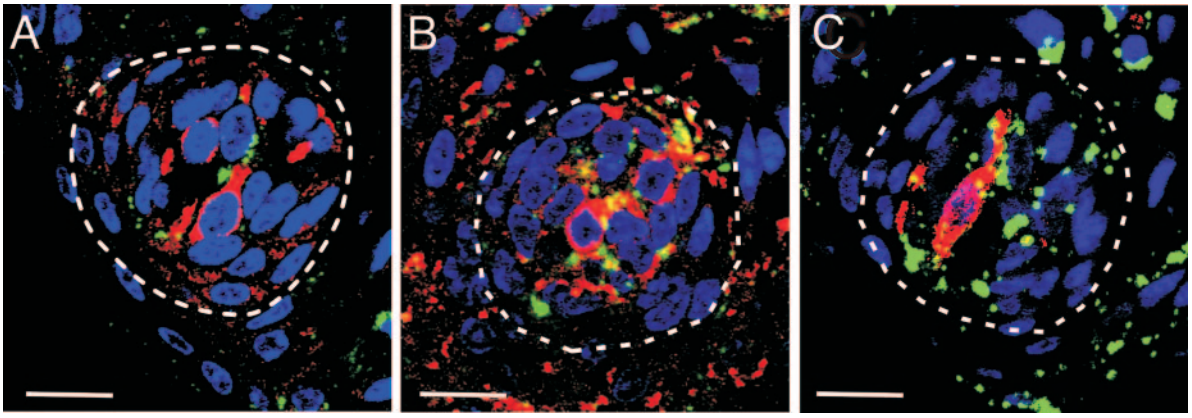

FIG. 3. Laser scanning confocal microscopy of taste buds in the fungiform papillae of hamsters intracerebrally inoculated with the HY TME agent. All images are oriented with the apical end of the taste bud toward the bottom left quadrant. The dashed line delineates taste bud boundaries. Dual immunofluorescence for PrP^{Sc} (A through C) labeled with Alexa Fluor 488 (green) and either α-gustducin (A), synaptobrevin-2 (B), or SNAP-25 (C), which were visualized using an anti-rabbit Alexa Fluor 568-conjugated antibody (red) on the same tissues. ToPro-3 (blue) was used as a nuclear counterstain. In taste cells, colocalization (yellow) of PrP^{Sc} and synaptobrevin-2 (B) or SNAP-25 (C) was observed, but no colocalization was seen in α-gustducin-positive taste cells (A) during the clinical phase of TME disease. Synaptobrevin-2 and SNAP-25 can also identify intragemmal and perigemmal nerve fibers, and colocalization with PrP^{Sc} could be present in these fibers as well as in taste cells. Bar, 20 μm. Images have an optical thickness of 0.8 μm.

colocalized with cytokeratin (Fig. 4C). Deconvolution and statistical analysis indicated that the MOCs for cytokeratin and PrP^{Sc} in mock-infected and HY TME-infected tongue samples were different ($P < 0.001$, Student's t test) (Table 2), and the M2 coefficient in the SSE of HY TME-infected hamsters indicated that 95% of the PrP^{Sc} in the SSE overlapped with cytokeratin-positive cells. The colocalization analyzer tool of the Huygens Essential software allowed visualization of colocalized areas within the tissue following deconvolution. Regions within the image in which the degree of colocalization exceeded a threshold became objects, and these colocalized objects appeared yellow, while the noncolocalized areas appeared as shades of gray. Punctate yellow deposits were present in the apical region of the stratum granulosum of HY TME-infected fungiform papillae (Fig. 4D). No colocalization of PrP^{Sc} with SNAP-25 or synaptobrevin-2 was found in the SSE (Table 2).

Our earlier results revealed that 73% of the PrP^{Sc} located in the SSE of fungiform papillae was colocalized with PGP 9.5-positive nerve fibers (Fig. 2C and Table 2); therefore, it is difficult to reconcile our findings that 95% of PrP^{Sc} in the SSE also colocalized with cytokeratin. Since cytokeratin immunofluorescence was uniformly distributed throughout the SSE (Fig. 4A) and PGP 9.5 had a more focal pattern in the SSE (Fig. 2A), an additional colocalization experiment was performed in order to determine if LSCM could discriminate between nerve fibers and cytokeratin-positive cells in the SSE. LSCM was initially used to demonstrate that a monoclonal anti-PGP 9.5 antibody and a polyclonal anti-PGP 9.5 antibody labeled the same structures in the SSE (M2 = 0.99; data not shown). LSCM for PGP 9.5 and cytokeratin in the SSE of fungiform papillae revealed that 99% of the PGP 9.5 colocalized with cytokeratin. This finding suggested that LSCM was unable to discriminate nerve fibers and epithelial cells in the SSE as distinct structures. Additional ultrastructural studies will be necessary to determine the spatial relationship of this PrP^{Sc} population with epithelial cells in the SSE.

The centrifugal spread of the prion agent was also investigated in the nasal cavity of hamsters that were i.c. inoculated with the HY TME agent. At the clinical stage of disease, PrP^{Sc} immunostaining was prominent in the olfactory sensory epithelium of the main nasal cavity, but was not found in the respiratory epithelium (Fig. 5A). Olfactory and respiratory epithelia were distinguished based on their histological characteristics in hematoxylin-and-eosin-stained sections and the presence of PGP 9.5 immunostaining in the olfactory sensory epithelium but not the respiratory epithelium (data not shown). In the olfactory sensory epithelium, PrP^{Sc} was found in the cell layers containing the olfactory sensory neurons and support cells. The PrP^{Sc} deposition pattern in the nasal cavity appeared to be in the dendritic knobs of olfactory sensory neurons and, less frequently, within the dendrites between these nerve cell bodies and their dendritic terminals (Fig. 5A). Within the nasal septum, PrP^{Sc} immunostaining was present in the vomeronasal organ, where it was found in the vomeronasal sensory epithelium but not in the nonsensory epithelium (Fig. 5B). The PrP^{Sc} deposition pattern in the vomeronasal sensory epithelium was remarkably similar to that in the olfactory sensory epithelium; the majority of the PrP^{Sc} was located in the epithelial cell layer containing sensory neurons, as well as at the apical ends of the dendrites, which form microvilli at the mucosal surface. In Fig. 5B, PrP^{Sc} immunostaining of the microvilli of vomeronasal sensory neurons was clearly demarcated from ciliated nonsensory epithelia, which do not exhibit PrP^{Sc} immunostaining. PrP^{Sc} deposition was also found in the olfactory bulbs of hamsters that were i.c. inoculated with the HY TME agent; however, PrP^{Sc} immunostaining in the olfactory nerves in the nasal cavity was very infrequent (data not shown) compared to PrP^{Sc} deposition in nerve fascicles in the tongue (Fig. 1E). Mucosal epithelium in the main nasal cavity or vomeronasal organ from mock-infected hamsters did not exhibit PrP^{Sc}-positive immunostaining (Fig. 5C). Lastly, PrP^{Sc} deposits were also found in the nasal-associated lymphoid tissue that has a subepithelial distribution in the nasal cavity (Fig. 5D).

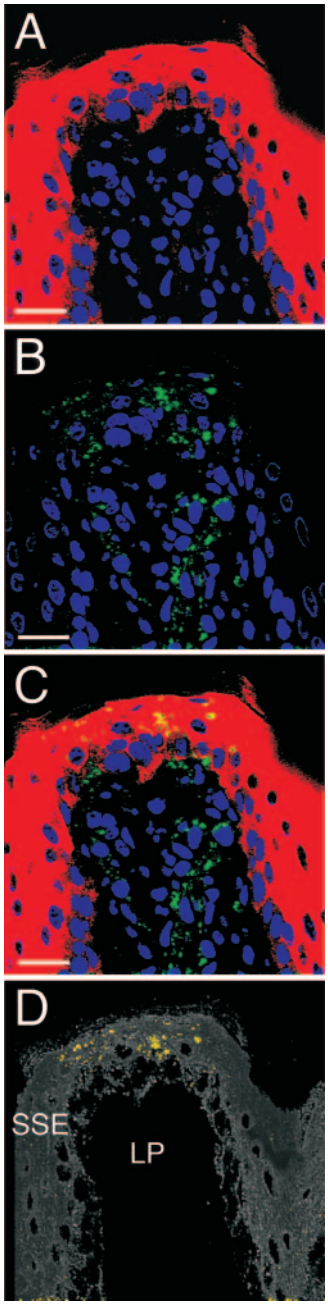

FIG. 4. Laser scanning confocal microscopy for PrP^{Sc} and cytokeratin in fungiform papillae of hamsters intracerebrally inoculated with the HY TME agent. Immunofluorescence images (optical thickness, 0.8 μm) for cytokeratin (A, red) and PrP^{Sc} (B, green) were merged in order to investigate areas of overlap (C, yellow). Colocalization of PrP^{Sc} and cytokeratin was found in the stratified squamous epithelium during the clinical phase of TME disease. Deconvolution and colocalization analysis of a *z* stack (i.e., a compiled stack of images acquired at 0.25-μm intervals through the thickness of the tissue) through the area shown in panels A through C illustrates only areas of colocalization (yellow) between cytokeratin and PrP^{Sc} (D). LP, lamina propria. Bar, 20 μm.

DISCUSSION

In this study we demonstrate that PrP^{Sc} accumulates in the taste buds of fungiform papillae in the tongue following intracerebral inoculation, which is consistent with spread of the HY TME agent from the brain stem to the tongue along sensory nerve fibers (Fig. 6). In the taste bud, during the clinical phase of disease, PrP^{Sc} colocalized with SNAP-25, a marker for type III taste cells but did not localize with α-gustducin, a marker for type II taste cells. Taste buds in fungiform papillae are innervated by the chorda tympani branch of the facial nerve. These gustatory nerve fibers have been shown to synapse with type II and type III taste cells in murine tongue (18, 40), while in the rat, only type III taste cells have been shown to synapse with sensory nerve fibers (64). Our findings of PrP^{Sc} accumulation in type III but not type II taste cells in hamsters would be consistent with the innervation pattern of the rat if HY TME infection of type III taste cells is dependent on synaptic contact with the chorda tympani nerve. Antibodies to markers for type I taste cells were not effective in the hamster tissue, so we could not determine the status of HY TME infection in these taste cells. Prion infection of taste buds has not been previously described, but a loss of taste and smell was reported to be a presenting symptom in a case of variant Creutzfeldt-Jakob disease, suggesting involvement of the gustatory and olfactory systems in prion-induced neurodegeneration (44). In the brain stem, the rostral portion of the nucleus of the solitary tract (NST) is involved in gustatory function; this nucleus is a target for prion infection in scrapie in sheep (17, 31, 45), CWD in deer (48), and bovine spongiform encephalopathy in cattle (56, 57). Based on our findings that HY TME agent infection in the brain stem can spread to taste buds via sensory nerves that synapse in this nucleus, it will be necessary to investigate whether the prion agent can also spread to the taste buds in ruminants.

HY TME infection at time of clinical disease was also found in nerve fibers throughout the tongue, including the lamina propria and SSE of fungiform papillae. In the lamina propria, LSCM analysis indicated that 78% of PrP^{Sc} was located in nerve fibers, especially in the subgemmal plexus. This finding is consistent with the spread of the HY TME agent to taste cells along gustatory fibers of the tongue (Fig. 6). Prior studies have reported prion agent infection in nerve fibers in the lamina propria of fungiform papillae in experimental TME infection (39) and in the fungiform and circumvallate papillae in sheep with natural scrapie (14), which is consistent with centrifugal spread via the chorda tympani branch of the facial nerve.

The current findings also demonstrated that 73% of PrP^{Sc} deposition in the SSE of fungiform papillae was colocalized to nerve fibers that were located perigemmal to taste buds as well as extragemmal at the apical region of the SSE. This distribution of the HY TME agent is consistent with spread from the brain stem to the SSE via somatosensory fibers of the lingual branch of the mandibular division of the trigeminal nerve (Fig. 6). Prion infection of the trigeminal ganglion has been reported in sheep with scrapie (52), cattle with bovine spongiform encephalopathy (55), and humans with vCJD (25), which supports the hypothesis that centrifugal spread of the prion agent in the trigeminal nerve could lead to prion infection in somatosensory nerves of the SSE in humans or ruminants with prion disease.

Colocalization of PrP^{Sc} and cytokeratin revealed extensive overlap in the SSE of HY TME-infected hamsters. This was an unexpected finding, since prion infection of epithelial cells in vivo has not been described, although PrP^{C} expression has

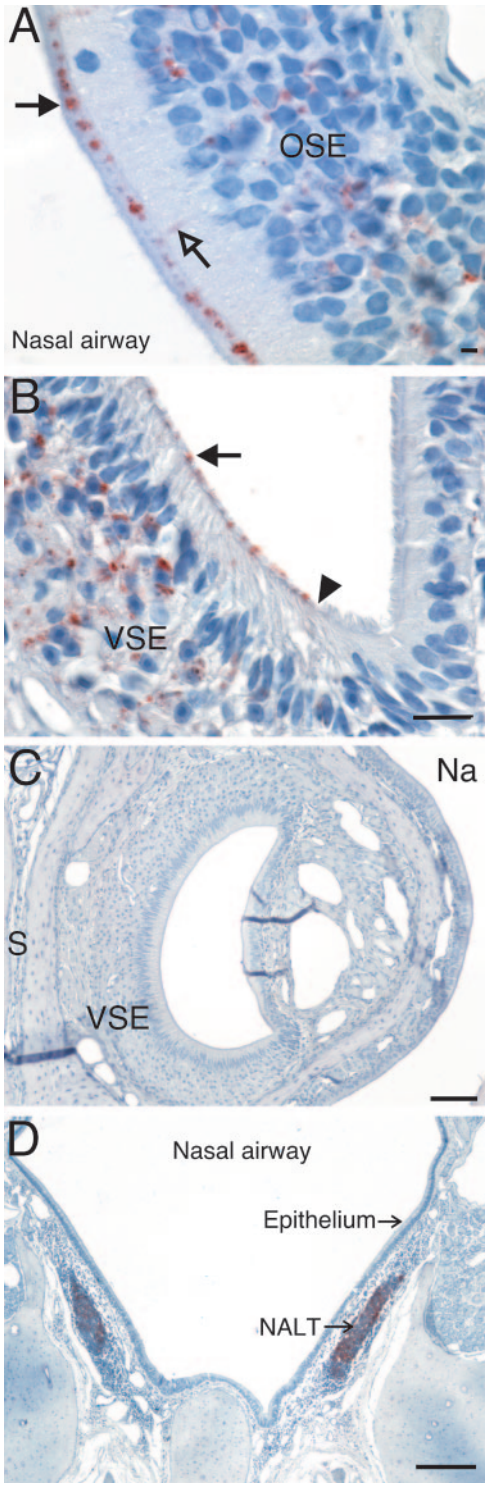

FIG. 5. PrP^{Sc} distribution in the nasal cavity following intracerebral inoculation of the HY TME agent. Mock-infected (C) and clinical HY TME-infected (A, B, and D) hamsters were analyzed for prion infection at time of clinical disease using PrP^{Sc} immunohistochemistry as described in Materials and Methods. (A) PrP^{Sc} deposition was found in the olfactory sensory epithelium (OSE) where it was associated with the cell body layer, dendrites (open arrow), and dendritic terminals (filled arrow). In the vomeronasal organ (B), PrP^{Sc} was present in the vomeronasal sensory epithelium (VSE) but not the nonsensory epithelium. There was a demarcation (filled arrowhead) between the PrP^{Sc} deposits at the dendritic terminals near the mucosal surface of the VSE (filled arrow) and the ciliated nonsensory epithelium. PrP^{Sc} was also observed in the nasal-associated lymphoid tissue (NALT) in the nasal cavity (D). PrP^{Sc} immunostaining was not apparent in the nasal epithelium or vomeronasal organ from mock-infected hamsters (C). S, septum; Na, nasal airway. Bars: panel A, 200 μm; panel B, 20 μm; panel C, 200 μm; panel D, 20 μm.

been documented in the tongues of sheep (37) as well as the squamous epithelium of the upper gastrointestinal tract and skin of bovines (41). Although >95% of PrP^{Sc} colocalized with the cytokeratin immunofluorescence signal in the SSE of HY TME-infected hamsters, these results should be cautiously interpreted for the following reasons. (i) Unlike PGP 9.5 immunofluorescence in the SSE, where well-defined nerve fibers were identified, cytokeratin immunofluorescence was uniformly distributed throughout the stratum granulosum and stratum corneum. This produced an immunofluorescence pattern in the SSE that was continuous from the edge of the lamina propria to the apical keratin layer, except for an absence of immunofluorescence in nuclei. (ii) Approximately three-quarters of PrP^{Sc} colocalized with the PGP 9.5 immunofluorescence and with 95% of the cytokeratin immunofluorescence in the SSE. Although PrP^{Sc} analysis with each of these cell markers was not performed on the same tissue section using LSCM, it is mathematically incongruous that such a high percentage of PrP^{Sc} could be present in both of these structures in the SSE. (iii) LSCM for PGP 9.5 and cytokeratin revealed that 99% of PGP 9.5 immunofluorescence colocalized with cytokeratin in the SSE. For these reasons, our findings suggest that LSCM cannot discriminate immunofluorescence signals between nerve fibers and epithelial cells. Therefore, LSCM may not be able to spatially distinguish PrP^{Sc} that is located in a nerve fiber from an epithelial cell when colocalization with cytokeratin is performed. Unlike the high M2 coefficient (0.95) for PrP^{Sc} and cytokeratin in the SSE of HY TME-infected hamsters, 27% of the PrP^{Sc} signal did not colocalize with PGP 9.5 in the SSE (M2 = 0.73, Table 2). We interpret these findings to indicate that the majority of PrP^{Sc} in the SSE was found in the well-defined nerve fibers, but a subpopulation of PrP^{Sc} in the SSE does not colocalize with nerve fibers. Despite our results showing a high degree of colocalization of PrP^{Sc} and cytokeratin by LSCM, even in ultrathin slices (0.05 μm) (data not shown), confirmation of PrP^{Sc} in epithelial cells will require additional studies.

Prion infection in the nasal cavity has previously been described in sporadic CJD where PrP^{Sc} deposition was reported in the central olfactory pathway (65). This study demonstrated PrP^{Sc} in the olfactory epithelium, including basal cells and cilia of olfactory neurons, as well as in the olfactory tract and bulb. Our findings of PrP^{Sc} deposition in the olfactory sensory epithelium but not the respiratory epithelium of hamsters infected with the HY TME agent are similar to those described in sporadic CJD. However, in the current study there was a paucity of PrP^{Sc} in the olfactory nerve, even though PrP^{Sc} was present in the olfactory bulb of HY TME-infected hamsters. This was in contrast to the distribution of PrP^{Sc} in nerve fibers of the tongue, where PrP^{Sc} deposits were found in fibers of the lamina propria, taste bud, and SSE of fungiform papillae and

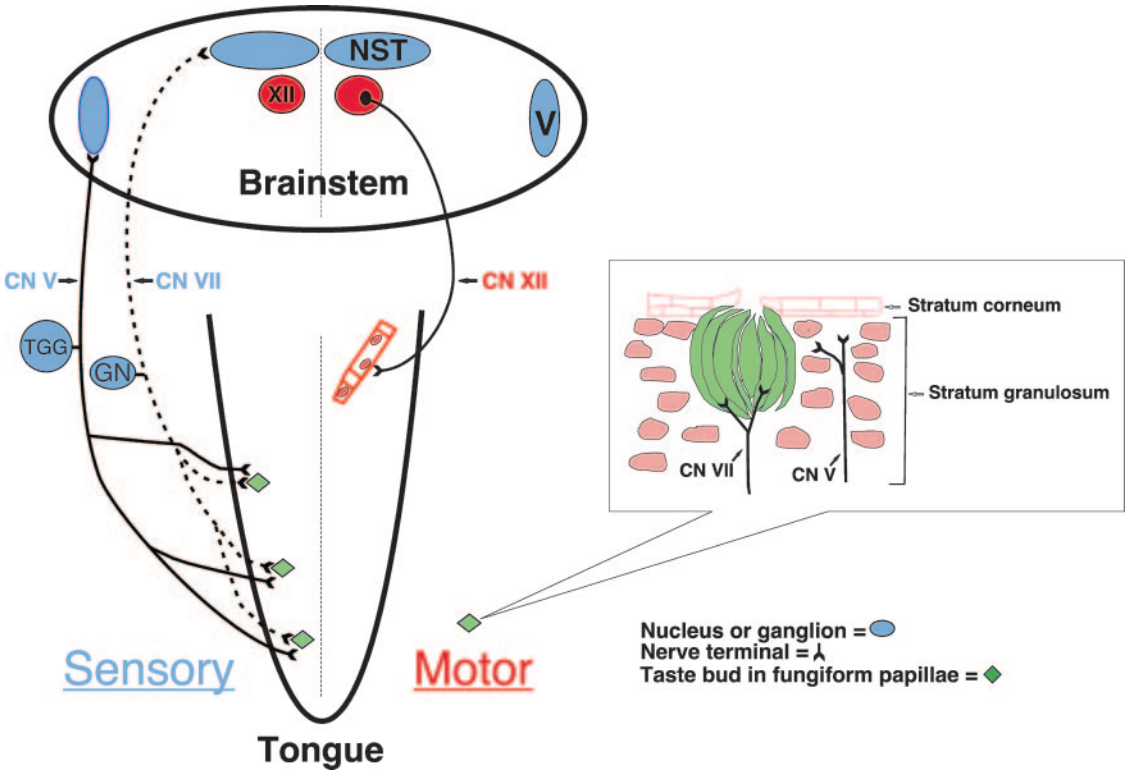

FIG. 6. Model for centrifugal spread of the HY TME agent from the brain stem to the tongue. The deposition of PrP^{Sc} in taste cells and the stratified squamous epithelium following intracerebral inoculation with the HY TME agent is consistent with centrifugal spread from the brain stem to the tongue via the chorda tympani branch of the facial nerve (CN VII) and the lingual branch of the mandibular division of the trigeminal nerve (CN V), respectively. The cell bodies for these two cranial nerves are located in the geniculate ganglion (GN) and the trigeminal ganglion (TGG), respectively. The central processes of the axons that convey taste information (i.e., in CN VII) terminate in the NST. The central processes of the axons that convey the general sensory information (i.e., in CN V) from the epithelium and muscles terminate in the principal and spinal trigeminal nucleus (V). Centrifugal spread of the HY TME agent to the tongue along these cranial nerves would likely require prion agent infection of NST or V nucleus and subsequent transsynaptic spread to nerve terminals in CN V and CN VII. The inset diagram illustrates a taste bud within the stratified squamous epithelium of a fungiform papilla. CN VII innervates a subset of taste cells within the taste bud, while branches of CN V ascend apically in the stratified squamous epithelium of the fungiform papilla. In addition, HY TME agent deposition in skeletal muscle cells is consistent with infection of motor neurons in the hypoglossal nucleus (XII) and retrograde transport within the hypoglossal nerve (CN XII). HY TME infection of either skeletal muscle cells or taste cells could be due to transsynaptic spread from CN XII or CN VII, respectively.

in fibers of the tongue parenchyma. Centrifugal spread of the HY TME agent from the olfactory bulbs to the olfactory sensory neurons in the epithelium along the olfactory nerve may not result in detectable levels of PrP^{Sc} accumulation, possibly due to lower levels of agent replication in the olfactory system compared to the gustatory system. Alternatively, olfactory receptor neurons undergo constant turnover and can be short-lived, which may preempt the buildup of PrP^{Sc} in olfactory axons of the hamster. Additionally, in the current study we did not have evidence for colocalization of PrP^{Sc} to cilia in the nasal cavity, but at the mucosa PrP^{Sc} had a distribution pattern consistent with spread along dendrites to dendritic knobs of the olfactory sensory neurons. The other major site of PrP^{Sc} deposition in the nasal cavities of HY TME-infected hamsters was the vomeronasal organ, specifically in the vomeronasal sensory epithelium. This distribution pattern is consistent with centrifugal spread of the HY TME agent from the olfactory bulb to the vomeronasal sensory neurons via the vomeronasal nerve. Although the respiratory and nonsensory epithelia in the nasal and vomeronasal organ mucosa, respectively, receive somatosensory innervation from the trigeminal nerve, centrifugal spread along this pathway does not appear to result in PrP^{Sc} deposition at these mucosal surfaces. Additionally, it has been reported that homogenates of nasal mucosa from sheep and goats experimentally inoculated with scrapie also contain prion infectivity (22, 23).

Our findings indicate that HY TME infection in the brain can undergo centrifugal spread along cranial nerves to the oral and nasal mucosa. HY TME infection of taste buds is consistent with transganglionic transport in the chorda tympani and synaptic spread to neuroepithelial taste cells, while transganglionic spread via the lingual nerve resulted in HY TME infection of somatosensory nerve fibers in the SSE of fungiform papillae. This latter pathway may have resulted in prion spread to epithelial cells in the SSE (Fig. 6). Similarly, HY TME infection of olfactory or vomeronasal sensory neuron cell bodies in the olfactory epithelium is consistent with retrograde spread to the neurons from the terminals located in the main or accessory olfactory bulbs, respectively. The prominent PrP^{Sc} deposition at the mucosal edge of the sensory epithelium is consistent with HY TME agent spread to the dendritic knobs of the olfactory sensory neurons. Since taste cells (15, 20),

epithelial cells (28), and olfactory sensory neurons (13, 19) undergo continuous renewal and turnover, prion infection of the oral and nasal mucosae of ruminants could play a role in the shedding of these prion-infected cells in mucus and saliva. In this scenario, horizontal prion transmission could be enhanced by the exchange of these bodily fluids via grazing, grooming, and mating behaviors, as well as in the later stages of CWD infection when hypersalivation is a clinical manifestation. A single attempt to detect prion infectivity in the saliva of a scrapie-infected goat was unsuccessful despite the presence of infectivity in the salivary gland. Recent improvements in bioassays and immunoassays for the prion agent have become available since this study was published over 30 years ago (22).

ACKNOWLEDGMENTS

This work was supported by Public Health Service grant R01 AI-055043 from the National Institute of Allergy and Infectious Diseases; by the National Research Initiative of the USDA Cooperative State Research, Education, and Extension Service, grant number 2006-35201-16626; by U.S. Fish and Wildlife Service grant 1448-60181-03-G739; and by NIH grant P20 RR-020185-01 from the National Center for Research Resources.

Special thanks go to Becca Sorg and Lisa Hughes for excellent technical assistance, to Renee Arens for animal care, and to Anthony Kincaid for critical reading of the manuscript.

REFERENCES

1. **Andreoletti, O., P. Berthon, D. Marc, P. Sarradin, J. Grosclaude, L. van Keulen, F. Schelcher, J. M. Elsen, and F. Lantier.** 2000. Early accumulation of PrP(Sc) in gut-associated lymphoid and nervous tissues of susceptible sheep from a Romanov flock with natural scrapie. J. Gen. Virol. **81:**3115–3126.
2. **Andreoletti, O., C. Lacroux, A. Chabert, L. Monnereau, G. Tabouret, F. Lantier, P. Berthon, F. Eychenne, S. Lafond-Benestad, J. M. Elsen, and F. Schelcher.** 2002. PrP(Sc) accumulation in placentas of ewes exposed to natural scrapie: influence of foetal PrP genotype and effect on ewe-to-lamb transmission. J. Gen. Virol. **83:**2607–2616.
3. **Andreoletti, O., S. Simon, C. Lacroux, N. Morel, G. Tabouret, A. Chabert, S. Lugan, F. Corbiere, P. Ferre, G. Foucras, H. Laude, F. Eychenne, J. Grassi, and F. Schelcher.** 2004. PrPSc accumulation in myocytes from sheep incubating natural scrapie. Nat. Med. **10:**591–593.
4. **Bartz, J. C., C. DeJoia, T. Tucker, A. E. Kincaid, and R. A. Bessen.** 2005. Extraneural prion neuroinvasion without lymphoreticular system infection. J. Virol. **79:**11858–11863.
5. **Bartz, J. C., A. E. Kincaid, and R. A. Bessen.** 2003. Rapid prion neuroinvasion following tongue infection. J. Virol. **77:**583–591.
6. **Beekes, M., and P. A. McBride.** 2000. Early accumulation of pathological PrP in the enteric nervous system and gut-associated lymphoid tissue of hamsters orally infected with scrapie. Neurosci. Lett. **278:**181–184.
7. **Beekes, M., P. A. McBride, and E. Baldauf.** 1998. Cerebral targeting indicates vagal spread of infection in hamsters fed with scrapie. J. Gen. Virol. **79:**601–607.
8. **Bessen, R. A., and R. F. Marsh.** 1994. Distinct PrP properties suggest the molecular basis of strain variation in transmissible mink encephalopathy. J. Virol. **68:**7859–7868.
9. **Bessen, R. A., and R. F. Marsh.** 1992. Identification of two biologically distinct strains of transmissible mink encephalopathy in hamsters. J. Gen. Virol. **73:**329–334.
10. **Borchelt, D. R., V. E. Koliatsos, M. Guarnieri, C. A. Pardo, S. S. Sisodia, and D. L. Price.** 1994. Rapid anterograde axonal transport of the cellular prion glycoprotein in the peripheral and central nervous systems. J. Biol. Chem. **269:**14711–14714.
11. **Boughter, J. D., Jr., D. W. Pumplin, C. Yu, R. C. Christy, and D. V. Smith.** 1997. Differential expression of alpha-gustducin in taste bud populations of the rat and hamster. J. Neurosci. **17:**2852–2858.
12. **Buschmann, A., and M. H. Groschup.** 2005. Highly bovine spongiform encephalopathy-sensitive transgenic mice confirm the essential restriction of infectivity to the nervous system in clinically diseased cattle. J. Infect. Dis. **192:**934–942.
13. **Carr, V. M., and A. I. Farbman.** 1992. Ablation of the olfactory bulb upregulates the rate of neurogenesis and induces precocious cell death in olfactory epithelium. Exp. Neurol. **115:**55–59.
14. **Casalone, C., C. Corona, M. I. Crescio, F. Martucci, M. Mazza, G. Ru, E. Bozzetta, P. L. Acutis, and M. Caramelli.** 2005. Pathological prion protein in the tongues of sheep infected with naturally occurring scrapie. J. Virol. **79:**5847–5849.
15. **Delay, R. J., J. C. Kinnamon, and S. D. Roper.** 1986. Ultrastructure of mouse vallate taste buds. II. Cell types and cell lineage. J. Comp. Neurol. **253:**242–252.
16. **Duffy, P., J. Wolf, G. Collins, A. G. DeVoe, B. Streeten, and D. Cowen.** 1974. Possible person-to-person transmission of Creutzfeldt-Jakob disease. N. Engl. J. Med. **290:**692–693. (Letter.)
17. **Ersdal, C., M. J. Ulvund, S. L. Benestad, and M. A. Tranulis.** 2003. Accumulation of pathogenic prion protein (PrPSc) in nervous and lymphoid tissues of sheep with subclinical scrapie. Vet. Pathol. **40:**164–174.
18. **Farbman, A. I.** 1965. Fine structure of the taste bud. J. Ultrastruct. Res. **12:**328–350.
19. **Farbman, A. I.** 1990. Olfactory neurogenesis: genetic or environmental controls? Trends Neurosci. **13:**362–365.
20. **Farbman, A. I.** 1980. Renewal of taste bud cells in rat circumvallate papillae. Cell Tissue Kinet. **13:**349–357.
21. **Guiroy, D. C., S. K. Shankar, C. J. Gibbs, Jr., J. A. Messenheimer, S. Das, and D. C. Gajdusek.** 1989. Neuronal degeneration and neurofilament accumulation in the trigeminal ganglia in Creutzfeldt-Jakob disease. Ann. Neurol. **25:**102–106.
22. **Hadlow, W. J., C. M. Eklund, R. C. Kennedy, T. A. Jackson, H. W. Whitford, and C. C. Boyle.** 1974. Course of experimental scrapie virus infection in the goat. J. Infect. Dis. **129:**559–567.
23. **Hadlow, W. J., R. C. Kennedy, and R. E. Race.** 1982. Natural infection of Suffolk sheep with scrapie virus. J. Infect. Dis. **146:**657–664.
24. **Head, M. W., V. Northcott, K. Rennison, D. Ritchie, L. McCardle, T. J. Bunn, N. F. McLennan, J. W. Ironside, A. B. Tullo, and R. E. Bonshek.** 2003. Prion protein accumulation in eyes of patients with sporadic and variant Creutzfeldt-Jakob disease. Investig. Ophthalmol. Vis. Sci. **44:**342–346.
25. **Head, M. W., D. Ritchie, N. Smith, V. McLoughlin, W. Nailon, S. Samad, S. Masson, M. Bishop, L. McCardle, and J. W. Ironside.** 2004. Peripheral tissue involvement in sporadic, iatrogenic, and variant Creutzfeldt-Jakob disease: an immunohistochemical, quantitative, and biochemical study. Am. J. Pathol. **164:**143–153.
26. **Heckmann, J. G., C. J. Lang, F. Petruch, A. Druschky, C. Erb, P. Brown, and B. Neundorfer.** 1997. Transmission of Creutzfeldt-Jakob disease via a corneal transplant. J. Neurol. Neurosurg. Psychiatry **63:**388–390.
27. **Heggebo, R., C. M. Press, G. Gunnes, K. I. Lie, M. A. Tranulis, M. Ulvund, M. H. Groschup, and T. Landsverk.** 2000. Distribution of prion protein in the ileal Peyer's patch of scrapie-free lambs and lambs naturally and experimentally exposed to the scrapie agent. J. Gen. Virol. **81:**2327–2337.
28. **Hill, M. W.** 1984. The ultrastructure of the oral epithelium, p. 7–30. *In* J. Meyer, C. A. Squier, and S. J. Gerson (ed.), The structure and function of oral mucosa. Pergamon Press, Elmsford, N.Y.
29. **Hunter, N., J. Foster, A. Chong, S. McCutcheon, D. Parnham, S. Eaton, C. MacKenzie, and F. Houston.** 2002. Transmission of prion diseases by blood transfusion. J. Gen. Virol. **83:**2897–2905.
30. **Iwanaga, T., H. Han, H. Kanazawa, and T. Fujita.** 1992. Immunohistochemical localization of protein gene product 9.5 (PGP 9.5) in sensory paraneurons of the rat. Biomed. Res. **13:**225–230.
31. **Jeffrey, M., S. Martin, L. Gonzalez, S. J. Ryder, S. J. Bellworthy, and R. Jackman.** 2001. Differential diagnosis of infections with the bovine spongiform encephalopathy (BSE) and scrapie agents in sheep. J. Comp. Pathol. **125:**271–284.
32. **Kascsak, R. J., R. Rubenstein, P. A. Merz, M. Tonna-DeMasi, R. Fersko, R. I. Carp, H. M. Wisniewski, and H. Diringer.** 1987. Mouse polyclonal and monoclonal antibody to scrapie-associated fibril proteins. J. Virol. **61:**3688–3693.
33. **Manuelidis, L., I. Zaitsev, P. Koni, Z. Y. Lu, R. A. Flavell, and W. Fritch.** 2000. Follicular dendritic cells and dissemination of Creutzfeldt-Jakob disease. J. Virol. **74:**8614–8622.
34. **McBride, P. A., W. J. Schulz-Schaeffer, M. Donaldson, M. Bruce, H. Diringer, H. A. Kretzschmar, and M. Beekes.** 2001. Early spread of scrapie from the gastrointestinal tract to the central nervous system involves autonomic fibers of the splanchnic and vagus nerves. J. Virol. **75:**9320–9327.
35. **Miller, M. W., and E. S. Williams.** 2003. Prion disease: horizontal prion transmission in mule deer. Nature **425:**35–36.
36. **Miller, M. W., E. S. Williams, N. T. Hobbs, and L. L. Wolfe.** 2004. Environmental sources of prion transmission in mule deer. Emerg. Infect. Dis. **10:**1003–1006.
37. **Moudjou, M., Y. Frobert, J. Grassi, and C. La Bonnardiere.** 2001. Cellular prion protein status in sheep: tissue-specific biochemical signatures. J. Gen. Virol. **82:**2017–2024.
38. **Moya, K. L., R. Hassig, C. Creminon, I. Laffont, and L. Di Giamberardino.** 2004. Enhanced detection and retrograde axonal transport of PrPc in peripheral nerve. J. Neurochem. **88:**155–160.
39. **Mulcahy, E. R., J. C. Bartz, A. E. Kincaid, and R. A. Bessen.** 2004. Prion infection of skeletal muscle cells and papillae in the tongue. J. Virol. **78:**6792–6798.

40. **Murray, R. G.** 1986. The mammalian taste bud type III cell: a critical analysis. J. Ultrastruct. Mol. Struct. Res. **95:**175–188.
41. **Pammer, J., A. Suchy, M. Rendl, and E. Tschachler.** 1999. Cellular prion protein expressed by bovine squamous epithelia of skin and upper gastrointestinal tract. Lancet **354:**1702–1703.
42. **Race, R., A. Jenny, and D. Sutton.** 1998. Scrapie infectivity and proteinase K-resistant prion protein in sheep placenta, brain, spleen, and lymph node: implications for transmission and antemortem diagnosis. J. Infect. Dis. **178:** 949–953.
43. **Race, R., M. Oldstone, and B. Chesebro.** 2000. Entry versus blockade of brain infection following oral or intraperitoneal scrapie administration: role of prion protein expression in peripheral nerves and spleen. J. Virol. **74:**828–833.
44. **Reuber, M., A. S. Al-Din, A. Baborie, and A. Chakrabarty.** 2001. New variant Creutzfeldt-Jakob disease presenting with loss of taste and smell. J. Neurol. Neurosurg. Psychiatry **71:**412–413.
45. **Ryder, S. J., Y. I. Spencer, P. J. Bellerby, and S. A. March.** 2001. Immunohistochemical detection of PrP in the medulla oblongata of sheep: the spectrum of staining in normal and scrapie-affected sheep. Vet. Rec. **148:**7–13.
46. **Schlegel, R., S. Banks-Schlegel, and G. Pinkus.** 1980. Immunohistochemical localization of keratin in normal human tissues. Lab. Investig. **42:**91–96.
47. **Seeger, H., M. Heikenwalder, N. Zeller, J. Kranich, P. Schwarz, A. Gaspert, B. Seifert, G. Miele, and A. Aguzzi.** 2005. Coincident scrapie infection and nephritis lead to urinary prion excretion. Science **310:**324–326.
48. **Spraker, T. R., R. R. Zink, B. A. Cummings, M. A. Wild, M. W. Miller, and K. I. O'Rourke.** 2002. Comparison of histological lesions and immunohistochemical staining of proteinase-resistant prion protein in a naturally occurring spongiform encephalopathy of free-ranging mule deer (Odocoileus hemionus) with those of chronic wasting disease of captive mule deer. Vet. Pathol. **39:**110–119.
49. **Thomzig, A., C. Kratzel, G. Lenz, D. Kruger, and M. Beekes.** 2003. Widespread PrPSc accumulation in muscles of hamsters orally infected with scrapie. EMBO Rep. **4:**530–533.
50. **Valdez, R. A., M. J. Rock, A. K. Anderson, and K. I. O'Rourke.** 2003. Immunohistochemical detection and distribution of prion protein in a goat with natural scrapie. J. Vet. Diagn. Investig. **15:**157–162.
51. **Vanes, K., and P. Brandt.** 1985. Retardation of immunofluorescence during microscopy. J. Histochem. Cytochem. **33:**755–761.
52. **van Keulen, L., B. E. C. Schreuder, M. E. W. Vromans, J. P. M. Langeveld, and M. A. Smits.** 2000. Pathogenesis of natural scrapie in sheep. Arch. Virol. Suppl. **16:**57–71.
53. **van Keulen, L., B. E. C. Schreuder, M. E. W. Vromans, J. P. M. Langeveld, and M. A. Smits.** 1999. Scrapie-associated prion protein in the gastro-intestinal tract of sheep with natural scrapie. J. Comp. Pathol. **121:**55–63.
54. **van Keulen, L. J. M., B. E. C. Schreuder, R. H. Meloen, G. Mooij-Harkes, M. E. W. Vromans, and J. P. M. Langeveld.** 1996. Immunohistochemical detection of prion protein in lymphoid tissues of sheep with natural scrapie. J. Clin. Microbiol. **34:**1228–1231.
55. **Wells, G. A., S. A. Hawkins, R. B. Green, A. R. Austin, I. Dexter, Y. I. Spencer, M. J. Chaplin, M. J. Stack, and M. Dawson.** 1998. Preliminary observations on the pathogenesis of experimental bovine spongiform encephalopathy (BSE): an update. Vet. Rec. **142:**103–106.
56. **Wells, G. A., and J. W. Wilesmith.** 1995. The neuropathology and epidemiology of bovine spongiform encephalopathy. Brain Pathol. **5:**91–103.
57. **Wells, G. A., J. W. Wilesmith, and I. S. McGill.** 1991. Bovine spongiform encephalopathy: a neuropathological perspective. Brain Pathol. **1:**69–78.
58. **Whitehead, M. C., C. S. Beeman, and B. A. Kinsella.** 1985. Distribution of taste and general sensory nerve endings in fungiform papillae of the hamster. Am. J. Anat. **173:**185–201.
59. **Williams, E. S., and S. Young.** 1992. Spongiform encephalopathies in Cervidae. Rev. Sci. Tech. **11:**551–567.
60. **Wilson, P. O., P. C. Barber, Q. A. Hamid, B. F. Power, A. P. Dhillon, J. Rode, I. N. Day, R. J. Thompson, and J. M. Polak.** 1988. The immunolocalization of protein gene product 9.5 using rabbit polyclonal and mouse monoclonal antibodies. Br. J. Exp. Pathol. **69:**91–104.
61. **Yang, R., H. H. Crowley, M. E. Rock, and J. C. Kinnamon.** 2000. Taste cells with synapses in rat circumvallate papillae display SNAP-25-like immunoreactivity. J. Comp. Neurol. **424:**205–215.
62. **Yang, R., C. L. Stoick, and J. C. Kinnamon.** 2004. Synaptobrevin-2-like immunoreactivity is associated with vesicles at synapses in rat circumvallate taste buds. J. Comp. Neurol. **471:**59–71.
63. **Yang, R., S. Tabata, H. H. Crowley, R. F. Margolskee, and J. C. Kinnamon.** 2000. Ultrastructural localization of gustducin immunoreactivity in microvilli of type II taste cells in the rat. J. Comp. Neurol. **425:**139–151.
64. **Yee, C. L., R. Yang, B. Bottger, T. E. Finger, and J. C. Kinnamon.** 2001. "Type III" cells of rat taste buds: immunohistochemical and ultrastructural studies of neuron-specific enolase, protein gene product 9.5, and serotonin. J. Comp. Neurol. **440:**97–108.
65. **Zanusso, G., S. Ferrari, F. Cardone, P. Zampieri, M. Gelati, M. Fiorini, A. Farinazzo, M. Gardiman, T. Cavallaro, M. Bentivoglio, P. G. Righetti, M. Pocchiari, N. Rizzuto, and S. Monaco.** 2003. Detection of pathologic prion protein in the olfactory epithelium in sporadic Creutzfeldt-Jakob disease. N. Engl. J. Med. **348:**711–719.